Available online at www.sciencedirect.com
SCIENCE DIRECT®
Toxicology and Applied Pharmacology xx (2006) xxx–xxx
Toxicology and Applied Pharmacology
www.elsevier.com/locate/ytaap

Benzo[a]pyrene and glycine N-methyltransferse Interactions: Gene expression profiles of the liver detoxification pathway

Cheng-Ming Lee [a], Shih-Yin Chen [a], Yuan-Chii G. Lee [b,1], Chi-Ying F. Huang [b], Yi-Ming Arthur Chen [a,*]

[a] *Division of Preventive Medicine, Institute of Public Health, National Yang-Ming University, Shih-Pai District, Taipei, Taiwan 112*
[b] *Division of Molecular and Genomic Medicine, National Health Research Institutes, Taipei, Taiwan 115*

Received 30 September 2005; revised 22 November 2005; accepted 6 December 2005

Abstract

Benzo[a]pyrene (BaP) is one of many polycyclic aromatic hydrocarbons that have been identified as major risk factors for developing various cancers. We previously demonstrated that the liver cancer susceptibility gene glycine N-methyltransferase (GNMT) is capable of binding with BaP and protecting cells from BaP-7,8-diol 9,10-epoxide-DNA adduct formation. In this study, we used a cytotoxicity assay to demonstrate that the higher expression level of GNMT, the lower cytotoxicity occurred in the cells treated with BaP. In addition, a cDNA microarray containing 7,597 human genes was used to examine gene expression patterns in BaP-treated HepG2 (a liver cancer cell line that expresses very low levels of GNMT) and SCG2-1-1 (a stable HepG2 clone that expresses high levels of GNMT) cells. The results showed that among 6,018 readable HepG2 genes, 359 (6.0%) were up-regulated more than 1.5-fold and 768 (12.8%) were down-regulated. Overexpression of GNMT in SCG2-1-1 cells resulted in the down-regulation of genes related to the detoxification, kinase/phosphatase pathways, and oncogenes. Furthermore, real-time PCR was used to validate microarray data from 21 genes belonging to the detoxification pathway. Combining both microarray and real-time PCR data, the results showed that among 89 detoxification pathway genes analyzed, 22 (24.7%) were up-regulated and 6 (6.7%) were down-regulated in BaP-treated HepG2 cells, while in the BaP-treated SCG2-1-1 cells, 12 (13.5%) were up-regulated and 26 (29.2%) were down-regulated ($P < 0.001$). Therefore, GNMT sequesters BaP, diminishes BaP's effects to the liver detoxification pathway and prevents subsequent cytotoxicity.

Keywords: GNMT; DNA arrays; Benzo[a]pyrene; Gene expression; Detoxification pathway

Introduction

Polycyclic aromatic hydrocarbons (PAHs) are carcinogenic in many animal species. Following their conversion into dihydrodiol epoxides by cytochrome P450 1A1 and epoxide hydrolase, they attack DNA and form PAH-DNA adducts (Guengerich, 1992; Shimada et al., 1992; Josephy, 1997). The liver detoxification pathway is not a single reaction, but a process involving multiple reactions and agents. BaP-7,8-diol 9,10-epoxide (BPDE) is a highly reactive electrophilic metabolite of BaP and causes mutations and cytotoxicity in both prokaryotic and eukaryotic cells (Denissenko et al., 1999). Nucleotide excision repair (NER) genes serve as the predominant DNA repair mechanism for BPDE adducts (Lloyd and Hanawalt, 2000; Wani et al., 2000).

Glycine N-methyltransferase (GNMT), first described in guinea pig livers by Blumenstein and Williams (1963), comprises between 1 and 3% of cytosolic proteins in rabbit and rat livers. Through its involvement in cellular one-carbon metabolism, GNMT regulates the ratio of S-adenosylmethionine

Abbreviations: PAH, polycyclic aromatic hydrocarbon; BaP, Benzo[a]pyrene; CYP P450, cytochrome P450; BPDE, BaP-7,8-diol 9,10-epoxide; CRR, common reference RNA; GST, glutathione S-transferase; AKR, aldo-keto reductase; UGT, UDP glycosyltransferase; ALDH, aldehyde dehydrogenase; ADH, alcohol dehydrogenase; ABC, ATP-binding cassette; SULT, sulfotransferase; NQO, NAD(P)H:quinone oxidoreductases; AOX, aldehyde oxidase; CES1, carboxylesterase 1; ACAD, acyl-coA dehydrogenase; EPHX, epoxide hydrolase; MAO, monoamine oxidase; MGST, microsomal glutathione S-transferase.

* Corresponding author. Fax: +886 2 28270576.
E-mail address: arthur@ym.edu.tw (Y.-M.A. Chen).
[1] Current address: Graduate Institute of Medical Informatics, Taipei Medical University, Taipei, Taiwan 110.

0041-008X/$ - see front matter © 2006 Published by Elsevier Inc.
doi:10.1016/j.taap.2005.12.020

(SAM) to S-adenosylhomocysteine (SAH) by catalyzing sarcosine synthesis from glycine and SAM (Kerr, 1972). In the liver, GNMT serves as a major folate-binding protein (Cook and Wagner, 1984). We recently suggested that GNMT may protect cells from attacks by environmental carcinogens such as BaP through direct interaction (Chen et al., 2004). Since GNMT inhibits DNA-adduct formation, we hypothesized that it plays an important role in altering detoxification pathway gene expression profiles following BaP exposure. In this study, we used a cytotoxicity assay to demonstrate that the higher expression level of GNMT, the lower cytotoxicity occurred in the cells treated with BaP. Subsequently, we used both microarray and real-time PCR to compare the gene expression profiles, especially the liver detoxification pathway, in HepG2 and SCG2-1-1 cells treated with BaP.

Materials and methods

Cell lines and culture. We used the HepG2 human hepatoblastoma cell line (Aden et al., 1979) and the HepG2-derived SCG2-neg, -1-1, -1-11 cell lines in this study. The SCG2-neg was a stable clone transfected with the control vector plasmid DNA. SCG2-1-11 expressed low level of GNMT and SCG2-1-1 expressed relative high level of GNMT (Chen et al., 2004). Cells were cultured in Dulbecco's modified Eagle's medium (GIBCO BRL, Grand Island, NY) with 10% heat-inactivated fetal bovine serum (HyClone, Logan, Utah), penicillin (100 U/ml), streptomycin (100 μg/ml), nonessential amino acids (0.1 mM), fungizone (2.5 mg/ml) and L-glutamine (2 mM) in a humidified incubator with 5% CO_2. Hygromycin B (300 μg/ml) was added to the SCG2-neg, -1-1, -1-11 culture medium.

Cytotoxicity assay. The SCG2-neg, SCG2-1-1, and SCG2-1-11 were seeded in six-well culture plates (10,000 cells per well) and cultured overnight. Cells were treated with 1, 5 or 10 μM BaP as well as DMSO solvent for 14 days in triplicate. Following removal of the medium, the cells were rinsed twice with phosphate buffered saline (PBS) and fixed with 1.25% glutaraldehyde (Nacalai Tesque, Tokyo, Japan) in PBS for 30 min at room temperature. After two rinses with distilled water, 0.05% methylene blue solution was added to each well and incubated for 30 min at room temperature. After two rinses with distilled water, the plates were dried and the stained colonies were solubilized by adding 0.33 N HCl solution (1 ml per well). The optical density (OD) of the resultant reactions was determined at A630 using ELx808 reader (Bio-Tek, Winooski, VT).

BaP treatment and mRNA isolation. BaP was dissolved in DMSO. HepG2 and SCG2-1-1 cells were treated with DMSO or 10 μM BaP for 12 h, harvested, and immediately homogenized in TRIzol (Invitrogen, Carlsbad, CA) for RNA isolation. DNase-treated total RNA and Oligotex dt resin (Qiagen, Valencia, CA) were used to isolate mRNA, following the manufacturer's instructions. Common Reference RNAs (CRR) were used as a control by pooling equal quantities of total RNA from the following 31 cell lines: HS-68, H1155, H522, HeLa, SiHa, MCF-7, H184B5F5/M10, CCD-966SK, HepG2, Hep3B, CE81T/VGH, CE146T/VGH, T24, SW620, UB-09, HCT-116, Gbm8401, Bcm1, Scm1, OECM-1, Jurkat, Normal, Cx, 172, 183, TSGH 8301, E7, CAL-27, IMR-32, 293 and Huh-7.

Hybridization and analysis. Cy3- and Cy5-labeled cDNA targets were respectively used for CRR and experimental samples. Labeled targets were hybridized in triplicate with a commercial 7500 cDNA microarray chip (ABC Human UniversoChip 8 K; Asia BioInnovations Corporation, Taipei). Fluorescent intensities of the Cy3 and Cy5 targets were separately measured and scanned using a GenePix 4000 B Array Scanner (Axon, Foster City, CA). Data extraction was performed using GenePix Pro 3.0.5.56 (Axon). A GAPD gene found in several chip blocks was used for signal normalization. Following proposed standards for Minimum Information About a Microarray Experiment (MIAME) (Brazma et al., 2001), sample information, intensity measurements, error analysis, microarray content, and slide hybridization conditions are available at Gene Expression Omnibus (GEO) (http://www.ncbi.nlm.nih.gov/geo/).

Hierarchical clustering. Cluster 3.0 software (http://bonsai.ims.u-tokyo.ac.jp/~mdehoon/software/cluster/) was used to perform hierarchical clustering and to create self-organizing maps. Data were visualized for browsing with TreeView 1.6. (http://genome-www5.stanford.edu//resources/restech.shtml). The hierarchical clustering algorithm was based on Sokal and Michener's average-linkage method (Sokal and Michener, 1958), which they developed for clustering correlation matrixes. The algorithm is used to compute a dendrogram that places all elements on a single tree. Software for implementing the algorithm is available at http://rana.stanford.edu/clustering (Eisen et al., 1998).

Real-time PCR. Twenty-one genes belonging to the liver detoxification pathway were selected for real-time PCR analysis. Complementary DNA was produced from cellular RNA (5 μg) using a SuperScript II RNase H- Reverse Transcriptase Kit (Invitrogen, Carlsbad, CA). Real-time PCR primers were designed using PRIMER EXPRESS software (Version 1.5, Applied Biosystems) and verified the specificity of sequences using BLAST (http://www.ncbi.nlm.nih.gov/BLAST/). Reactions were performed in 10-μl quantities of diluted cDNA sample, primers (100, 200, or 300 nM), and a SYBR Green PCR Master Mix containing nucleotides, AmpliTaq Gold DNA polymerase, and optimized buffer components (Applied Biosystems). Reactions were assayed using an Applied Biosystems Prism 7700 sequence detection system.

After cycling, a melting curve was produced via the slow denaturation of PCR end products to validate amplification specificity. Predicted cycle threshold (C_T) values were exported into EXCEL worksheets for analysis. Comparative C_T methods were used to determine relative gene expression folds to GAPD. GNMT primers were used to confirm gene expression levels. Primers for detoxification pathway phase I, II and III genes were designed to validate the microarray data. Gene selection was based on cDNA array expression levels (i.e., high, medium, or low) and their relevance to the BaP treatment in the literatures. The BaP-inducible genes CYP1A1 and CYP1A2 were included in our measurements. The primers used for real-time PCR were shown as the followings: ABCB1-F (5′-GTCCCAGGAGCCCATCCT) and ABCB1-R (5′-CCCGGCTGTTGTCTCCATA) for ABCB1; ABCB6-F (5′-TTCAGAAGGGCCGTATTGAGTT) and ABCB6-R (5′-TGAAAGACACGTCCTGCAGAGT) for ABCB6; ABCB10-F (5′-CCCCAAGGGTTCAACACTGT) and ABCB10-R (5′-AATCGCAATCCGCTGTTTCT) for ABCB10; ACADSB-F (5′-TTAGAAGCTGGAAAGCCATTCAT) and ACADSB-R (5′-TACTCGTTGTTTGTCCTGCAATCT) for ACADSB; AKR1B10-F (5′-CCAGGTTCTGATCCGTTTCC) and AKR1B10-R (5′-ACAATGCGTGCTGGTGTCA) for AKR1B10; AKR1C1-F (5′-CACCAAATTGGCAATTGAAGCT) and AKR1C1-R (5′-AACCTGCTCCTCATTATTGTATAA) for AKR1C1; AKR1C2-F (5′-GCCGTCAAATTGGCAATAGAAG) and AKR1C2-R (5′-AACCTGCTCCTCATTATTGTAAAC) for AKR1C2; ALDH3A1-F (5′-GGAGCTGCTCAAGGAGAGGTT) and ALDH3A1-R (5′-GCAGCCGTCATGATGATCTTC) for ALDH3A1; CES1-F (5′-GCTGGAGCACCCACCTACA) and CES1-R (5′-CTCCTATCACCGTCTTGGGTTT) for CES1; CYP1A1-F (5′-GCTGCAACGGGTGGAATT) and CYP1A1-R (5′-CAGGCATGCTTCATGGTTAGC) for CYP1A1; CYP1A2-F (5′-GGAGCAGGATTTGACACAGTCA) and CYP1A2-R (5′-TTCCTCTGTATCTCAGGCTTGGT) for CYP1A2; CYP19-F (5′-AAGACGCAGGATTTCCACAGA) and CYP19-R (5′-TCTTGTCAGGTCACCACGTTTC) for CYP19; CYP39A1-F (5′-GGACCCATTACCCAAACAGAGTT) and CYP39A1-R (5′-TTTGTTTATATTCAATTCGGCATTG) for CYP39A1; EPHX1-F (5′-GGAGGCCTGGAAAGGAAGTT) and EPHX1-R (5′-TGATGGTGCCTGTTGTCCAGTA) for EPHX1; MGST2-F (5′-CAAAGTCAAGAAGCGCCATTT) and MGST2-R (5′-AGTTCCCGGCCATCTTTCTC) for MGST2; SULT1A3-F (5′-AGCCCAGGAGGTTGTGGATA) and SULT1A3-R (5′-TTGGAGGGAGGGTCTTGCTT) for SULT1A3; SULT2A1-F (5′-TTCGGCACGAGGTTGAAAC) and SULT2A1-R (5′-ACCATAAGAAATCGTCCGACATG) for SULT2A1; GNMT-F (5′-GCAGCCTTCGGAGGTAAGTG) and GNMT-R (5′-GGTTTGGCCTGGCTTGTAAG) for GNMT; GAPD-F (5′-TGGTATCGTGGAAGGACTCA) and GAPD-R (5′-AGTGGGTGTCGCTGTTGAAG) for GAPD.

Statistical analysis. Statistical analysis was performed using the SPSS 11.0 program. A Pearson chi-square test was used to compare gene expression profiles of BaP-treated HepG2 and SCG2-1-1 cells.

Results

Cytotoxicity of BaP on SCG2 cell lines

The SCG2 cell lines which including SCG2-neg, -1-11 and -1-1 cells were treated with DMSO, 5 or 10 μM BaP for 14 days and the cytotoxicity was determined through methylene blue staining and densitometry. The results shown that BaP caused dose-dependent cell death in the SCG2-neg. -1-11 and -1-1 cells (Fig. 1). If we assumed the optical density (OD) of the survived cells in the solvent control (DMSO) of each cell line as 100%, then the percentages of survived cells in SCG2-neg, SCG2-1-11 and SCG2-1-1 treated with 5 μM BaP were 47.0%, 52.6% and 60.5%, respectively; and the survived cells of SCG2-neg, -1-11 and -1-1 treated with 10 μM BaP were 15.8%, 24.2% and 37.5%, respectively. Therefore, the higher expression level of GNMT, the lower cytotoxicity occurred in the cells treated with BaP.

Microarray analysis of BaP effects on HepG2 cells

Triplicate microarray hybridization data results for each treatment were analyzed using EXCEL; GAPD levels were adjusted for each sample set. After deleting incorrect and skewed values, the data were normalized and averaged. Gene expression signals in BaP- and DMSO-treated HepG2 cells were compared. The results showed that the signals of 79.2% of the genes (6018 of 7597) were readable and fit for gene expression profile analysis.

Up-regulation was defined as a ratio of BaP to DMSO of 1.5 or greater; down-regulation was defined as a BaP-to-DMSO ratio of 0.67 or less. As shown in Table 1, 6.0% (359) of the readable genes were up-regulated following BaP treatment. The top three gene categories were cell matrix proteins (48), oncogenes (26) and transcription factors (26). The highest percentages of up-regulated genes were detoxification (13.9%), immune response (11.1%), and oncogenes (9.7%). Just over twice as many post-BaP treatment genes (768, or 12.8%) were down-regulated. Here, the top three categories were cell matrix proteins (84), transcription factors (76) and cell cycle genes (40). The highest percentages of down-regulated genes were in the categories of DNA repair (18.5%), cell cycle (18.3%), and tumor suppressors (16.3%) (Table 1).

Effects of GNMT overexpression in BaP-treated SCG2-1-1 cells

We extracted RNA from HepG2 and SCG2-1-1 cells treated with Ba or DMSO for microarray analysis. All cDNA microarray genes were analyzed by hierarchical clustering (Fig. 2A). Our results show that the gene expression profiles of DMSO-treated HepG2 and BaP-treated HepG2 cells had the most similarities and genes in middle sections of gene clusters were expressed at higher levels. In the presence of GNMT, BaP-treated SCG2-1-1 gene expression profiles were down-regulated on both sides of the gene clusters. Just under two-thirds (65%, or 4903/7597) of the cDNA signals were readable and fit for making comparisons. After BaP treatment, gene expression levels in every gene category decreased significantly in the SCG2-1-1 cells (Table 1). The largest percentages of decreased expression levels were noted in the detoxification (30.3%), kinase/phosphatase (29.4%), and oncogene (18.7%) categories.

Real-time PCR results

We used real-time PCR to verify gene expression profiles detected in the cDNA microarray. Since the cDNA microarray used in this study did not contain the GNMT gene, we also used

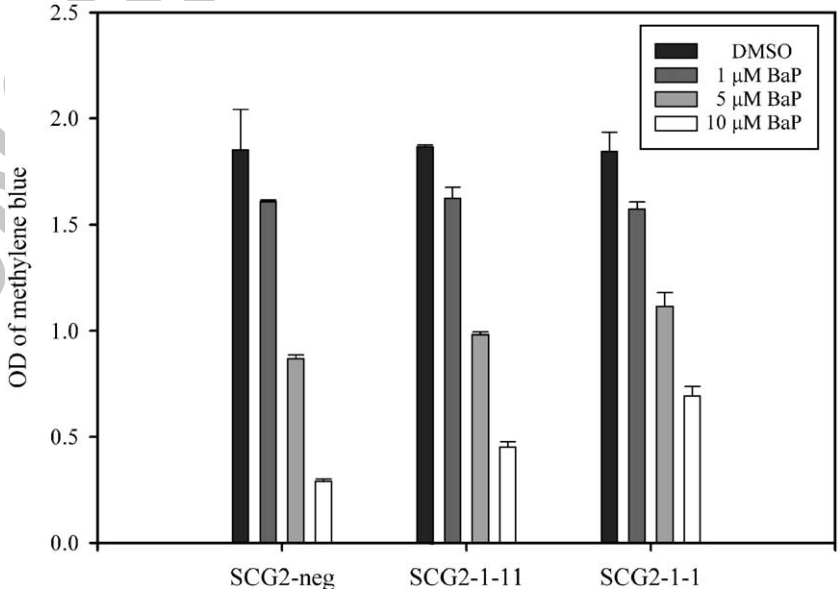

Fig. 1. Cytotoxicity assay. Cytotoxicity assays were determined by colorimetric analysis and the means ± SD of the **A630** were shown. The experiments were repeated once and similar results were obtained. Representative data are shown.

Table 1
Effects of gene expression profile induced by BaP in HepG2 and comparison between HepG2 and SCG2-1-1 cells

Gene category	HepG2 [a]		HepG2 [b]		SCG2-1-1		χ^2 Test [c] P value
	Induction [d,e]	Reduction [d,e]	Induction [d,e]	Reduction [d,e]	Induction [d,e]	Reduction [d,e]	
Detoxification (133)	13.9% (14/101)	8.9% (9/101)	14.6% (13/89)	6.7% (6/89)	11.2% (10/89)	29.2% (26/89)	<0.001
Oncogenes (327)	9.7% (26/269)	13.4% (36/269)	11.7% (25/214)	12.1% (26/214)	4.2% (9/214)	29.4% (63/214)	<0.001
Tumor suppressor (197)	4.2% (7/166)	16.3% (27/166)	5.2% (7/135)	14.8% (20/135)	3% (4/135)	30.4% (41/135)	<0.001
Apoptosis (255)	8.4% (19/225)	10.7% (24/225)	8.8% (17/194)	8.8% (17/194)	3.6% (7/194)	23.2% (45/194)	<0.001
Cell cycle (236)	4.1% (9/218)	18.3% (40/218)	4.7% (9/191)	17.8% (34/191)	2.6% (5/191)	38.2% (73/191)	<0.001
Transcription (588)	5.4% (26/483)	15.7% (76/483)	6.1% (25/407)	14.3% (58/407)	2.7% (11/407)	27.8% (113/407)	<0.001
DNA repair (89)	7.4% (6/81)	18.5% (15/81)	8.6% (6/70)	14.3% (10/70)	2.9% (2/70)	32.9% (23/70)	<0.001
Immune response (63)	11.1% (4/36)	11.1% (4/36)	9.4% (3/32)	12.5% (4/32)	3.1% (1/32)	25% (8/32)	<0.001
Signal transduction (483)	7.1% (22/311)	12.5% (39/311)	6.8% (16/236)	11.4% (27/236)	2.5% (6/236)	27.5% (65/236)	<0.001
DNA binding protein (149)	5.1% (7/138)	8.7% (12/138)	5.9% (7/118)	7.6% (9/118)	3.4% (4/118)	24.6% (29/118)	<0.001
Cell matrix protein (937)	6.4% (48/747)	11.2% (84/747)	7.2% (43/601)	9.5% (57/601)	2.7% (16/601)	23.6% (142/601)	<0.001
Structure protein (333)	3.9% (9/229)	13.1% (30/229)	4.8% (9/187)	10.2% (19/187)	0.5% (1/187)	24.6% (46/187)	<0.001
Kinase/Phosphatase (175)	6.9% (7/102)	10.8% (11/102)	7.1% (6/85)	11.8% (10/85)	3.5% (3/85)	27.1% (23/85)	<0.001
Other (2560)	6.3% (141/2244)	14.3% (320/2224)	7.0% (128/1837)	12.4% (227/1837)	2.7% (50/1837)	28.7% (527/1837)	<0.001
Unknown (1733)	4.5% (54/1193)	9.4% (112/1193)	5.2% (50/961)	7.6% (73/961)	2.5% (24/961)	25% (241/961)	<0.001
Total (7597)	6% (359/6018)	12.8% (768/6018)	6.6% (326/4903)	11.0% (541/4903)	2.7% (132/4903)	27.2% (1336/4903)	<0.001

[a] Used to analyze the effects of BaP on HepG2.
[b] Used to compare with SCG2-1-1.
[c] Chi-square test performed with 3 × 3 table; "no difference" category (ratio between 0.67 and 1.5) not shown.
[d] Induction: ratio of BaP treatment to DMSO 1.5 or more. Reduction: ratio 0.67 or less.
[e] Percentages based on readable genes in respective gene categories.

real-time PCR to measure GNMT expression levels. As shown in Table 2, GNMT expression levels in HepG2 cells were very low, and the expression levels in SCG2-1-1 cells were approximately 18 times greater; this was increased even further following BaP treatment. In addition, we used real-time PCR to confirm the expression levels of 21 of 89 genes belonging to the detoxification pathway. The real-time PCR/microarray results were quite compatible with five exceptions: CYP1A2, EPHX1, SULT1A3, SULT2A1 and UGT2B7. In all, 16 of 21 (76.2%) gene expression patterns from the cDNA microarray were validated.

Effects of GNMT–BaP interaction on liver detoxification pathway genes

In our microarrays, 133 genes belonged to the detoxification pathway. Of these, 89 (45 phase I, 28 phase II, and 16 phase III) were usable for studying the effects of GNMT–BaP interactions. After integrating the real-time PCR and microarray data, we observed that 25.9% (23/89) of the detoxification pathway genes were up-regulated and 5.6% (5/89) down-regulated in BaP-treated HepG2 cells. For the BaP-treated SCG2-1-1 cells the figures were 13.5% (12/89) up-regulated and 28.1% (25/89) down-regulated (Table 3). Among the 45 phase I genes, 13 (28.9%) were up-regulated and 3 (6.7%) down-regulated in HepG2 cells; 9 (20.0%) were up-regulated and 10 (22.2%) down-regulated in SCG2-1-1 cells ($P < 0.001$). Among the 28 phase II genes, 7 (25.0%) were up-regulated and 2 (7.1%) down-regulated in HepG2 cells; 2 (7.1%) were up-regulated and 9 (32.2%) were down-regulated in SCG2-1-1 cells ($P = 0.008$). Among the 16 phase III genes, 3 (18.8%) were up-regulated and zero were down-regulated in HepG2 cells; 1 (6.3%) was up-regulated and 6 (37.5%) down-regulated in SCG2-1-1 cells. We observed two gene expression profile clusters from our hierarchical clustering analysis of detoxification pathway genes: a) HepG2/DMSO and SCG2-1-1/DMSO, and b) HepG2/BaP and SCG2-1-1/BaP (Figs. 2B and C).

Six gene expression profile patterns in BaP-treated HepG2 and SCG2-1-1 cells

We identified 6 patterns among the gene expression profiles of BaP-treated HepG2 and SCG2-1-1 cells. As shown in Table 4 and Fig. 3, the A, C and F patterns indicate similarities in BaP responses in HepG2 and SCG2-1-1 genes. No differences were noted in pattern B gene expression levels for BaP-treated HepG2 and down-regulated SCG2-1-1 cells, including 7 phase I genes (CYP11B1, MAOA, AKR1A1, FMO5, ALDH3B2, CYP2C8 and CYP27B1), 6 phase II genes (ACADSB, GSTM2, UGT2B15, SULT4A1, TST and GSTM1), and 6 phase III genes (ABCC3, ABCD4, ABCF2, ABCB8, ABCF3 and ABCA3). In response to BaP treatment, only 1 gene (SULT2A1) was up-regulated in HepG2 and down-regulated in SCG2-1-1 cells (pattern D). The E pattern (up-regulated in HepG2 and no difference in SCG2-1-1) included 4 phase I (CYP2J2, CYP3A4, AKR1B1 and CES1), 4 phase II (MGST2, SULT1A3, GSTM3 and UGT2B7), and 2 phase III genes (ABCB10 and ABCB1). SCG2-1-1 cell expression ratios were down-regulated more than 2-fold in comparison with HepG2 cells in seven genes: CYP11B1, ACADSB, SULT2A1, MGST2, SULT1A3, UGT2B7 and ABCB10.

Nucleotide excision repair (NER) gene expression profiles

Since GNMT inhibits BPDE-DNA adduct formation (Chen et al., 2004), we hypothesized that genes involved in nucleotide

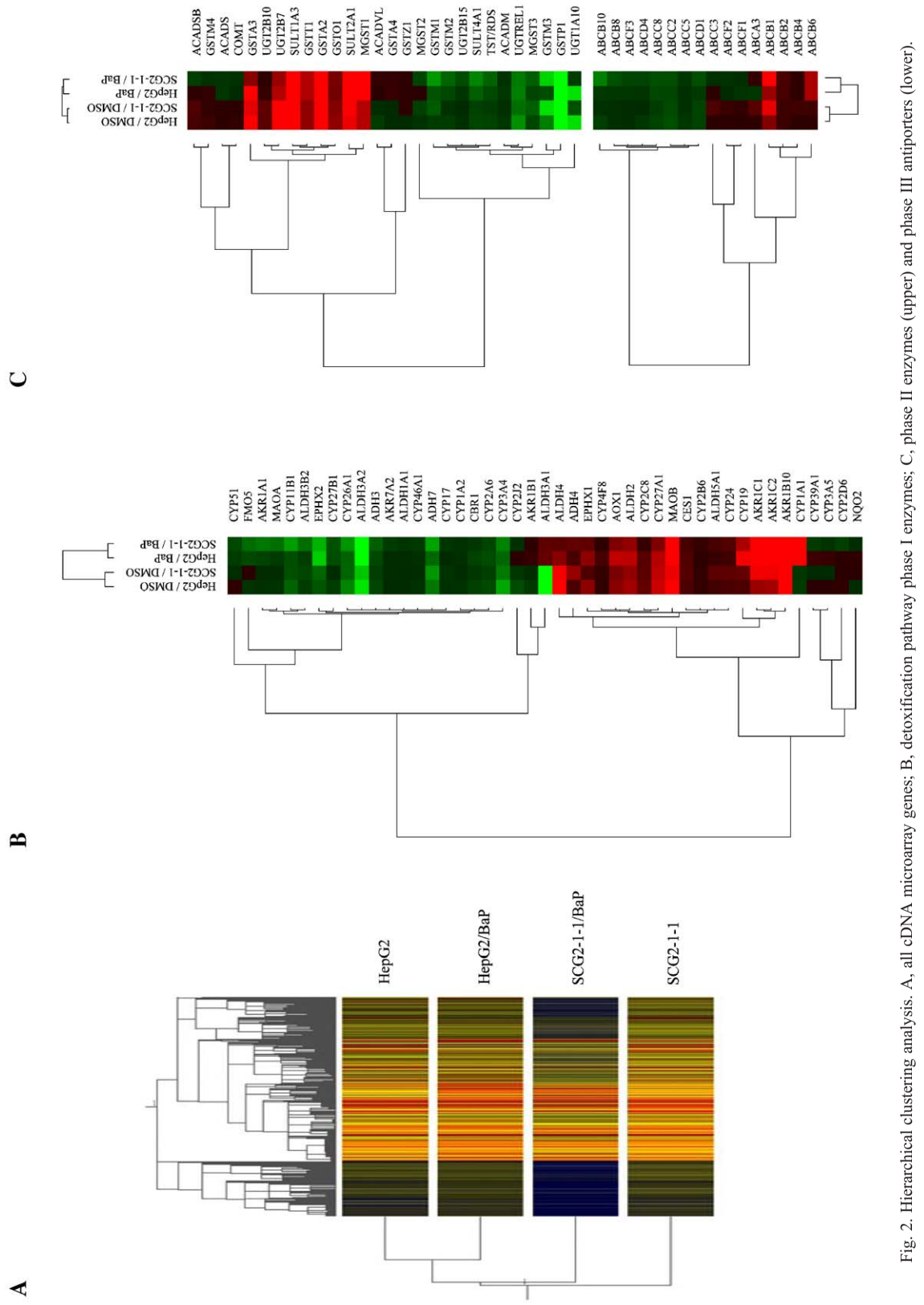

Fig. 2. Hierarchical clustering analysis. A, all cDNA microarray genes; B, detoxification pathway phase I enzymes; C, phase II enzymes (upper) and phase III antiporters (lower).

Table 2
Real-time PCR data for detoxification pathway genes

Gene	HepG2/DMSO	HepG2/BaP	SCG2-1-1/DMSO	SCG2-1-1/BaP	BaP/DMSO		Folds of reduction[a]
					HepG2	SCG2-1-1	
Phase I							
AKR1B10	0.95 ± 0.07	8.54 ± 1.88	2.19 ± 0.41	6.74 ± 1.51	8.99	3.08	2.9
AKR1C1	5.21 ± 0.03	28.71 ± 2.47	18.77 ± 2.16	56.43 ± 2.02	5.51	3.01	1.8
AKR1C2	1.63 ± 0.17	8.26 ± 1.12	3.87 ± 0.58	10.57 ± 0.49	5.06	2.73	1.9
ALDH3A1	0.03 ± 0.00	19.18 ± 0.20	0.04 ± 0.00	18.08 ± 0.31	762.71	460.91	1.7
CYP19	0.30 ± 0.02	1.32 ± 0.34	0.42 ± 0.08	0.74 ± 0.08	4.36	1.77	2.5
CYP1A1	0.17 ± 0.02	14.52 ± 0.50	0.38 ± 0.06	25.99 ± 0.63	85.23	68.75	1.2
CYP1A2	0.65 ± 0.07	2.16 ± 0.38	1.17 ± 0.13	3.36 ± 0.22	3.34	2.88	1.2
CYP2D6	0.07 ± 0.00	0.05 ± 0.02	0.03 ± 0.00	0.03 ± 0.00	0.74	0.82	0.9
CYP3A4[b]	2.40 ± 0.00	8.40 ± 0.80	0.80 ± 0.10	1.50 ± 0.30	3.51	1.83	1.9
CYP39A1	0.10 ± 0.02	0.42 ± 0.05	0.11 ± 0.02	0.21 ± 0.05	4.04	1.95	2.1
CES1	14.74 ± 1.4	23.56 ± 1.82	21.61 ± 0.09	27.57 ± 4.13	1.60	1.28	1.3
EPHX1	10.42 ± 0.79	20.99 ± 1.17	12.91 ± 0.32	19.9 ± 0.14	2.01	1.54	1.3
Phase II							
ACADSB	0.87 ± 0.04	1.16 ± 0.04	1.69 ± 0.09	0.87 ± 0.04	1.33	0.52	2.6
MGST2	0.42 ± 0.08	0.64 ± 0.12	0.59 ± 0.13	0.44 ± 0.15	1.53	0.76	2.0
SULT1A3	16.49 ± 0.64	45.36 ± 1.73	27.92 ± 1.16	35.96 ± 2.41	2.75	1.29	2.1
SULT2A1[b]	0.23 ± 0.15	0.40 ± 0.19	0.48 ± 0.11	0.16 ± 0.02	1.72	0.33	5.2
GSTM2	0.09 ± 0.02	0.12 ± 0.01	0.08 ± 0.00	0.03 ± 0.00	1.25	0.41	3.0
UGT2B7	0.12 ± 0.00	0.37 ± 0.03	0.13 ± 0.01	0.19 ± 0.00	3.10	1.48	2.1
Phase III							
ABCB1	8.98 ± 2.39	13.71 ± 1.29	15.78 ± 4.69	15.3 ± 0.28	1.53	0.97	1.6
ABCB10	0.44 ± 0.01	1.02 ± 0.03	0.92 ± 0.01	0.88 ± 0.02	2.31	0.96	2.4
ABCB6	0.71 ± 0.01	4.92 ± 0.19	1.43 ± 0.06	5.6 ± 0.90	6.93	3.91	1.8
ABCC3	0.06 ± 0.00	0.12 ± 0.01	0.12 ± 0.01	0.1 ± 0.00	1.89	0.86	2.2
GNMT	0.01 ± 0.00	0.02 ± 0.00	0.20 ± 0.02	1.76 ± 0.13	1.45	8.6	0.2

[c]Real-time PCR standardized with GAPD expression.
[a] Folds of reduction (GNMT effect) = (BaP/DMSO in HepG2)/(BaP/DMSO in SCG2-1-1).
[b] ×1000.

excision repair (NER) would be less active in BaP-treated SCG2-1-1 cells compared to BaP-treated HepG2 cells. We used microarrays to analyze the expression levels of six NER genes. ERCC1 (1.69- and 1.46-folds) was up-regulated and RAD23B (0.61- and 0.64-folds) was down-regulated in HepG2/BaP and SCG2-1-1/BaP cells. We also noted that DDB2 was increased 2.23-fold in HepG2/BaP cells but only 1.45-fold in SCG2-1-1/BaP cells.

Discussion

HepG2 cells retain morphological and biochemical characteristics of normal human hepatocytes (Aden et al., 1979; Knowles et al., 1980; Fukuda et al., 1992). In addition, HepG2 cells can activate BaP and other chemicals to genotoxic metabolites (Diamond et al., 1980; Dearfield et al., 1983; Limbosch, 1983; Diamond et al., 1984). Xenobiotic-metabolizing enzymes that have been demonstrated in HepG2 cells include cytochrome P450, NADPH-cytochrome c reductase, NADH-b_5 reductase, epoxide hydrase, and UDP-glucuronyl transferases (Dearfield et al., 1983; Sassa et al., 1987; Duthie et al., 1988; Grant et al., 1988). Since HepG2 cells express very small amounts of GNMT and a stable clone-SCG2-1-1 cells express abundant amounts of GNMT (Chen et al., 2004), we used these paired cell lines to investigate the effects of BaP on

Table 3
Effects of BaP treatment on detoxification pathway enzymes in HepG2 and SCG2-1-1 cells based on microarray and real-time PCR analyses

	HepG2			SCG2-1-1			χ^2 Test[a] *P* value
	Up	No difference	Down up	No	Difference	Down	
Phase I (*n* = 45)	13 (28.9%)	29 (64.4%)	3 (6.7%)	9 (20.0%)	26 (57.8%)	10 (22.2%)	<0.001
Phase II (*n* = 28)	7 (25.0%)	19 (67.9%)	2 (7.1%)	2 (7.1%)	17 (60.7%)	9 (32.2%)	0.008
Phase III (*n* = 16)	3 (18.8%)	13 (81.3%)	0 (0.0%)	1 (6.3%)	9 (56.3%)	6 (37.5%)	0.055
Total (*n* = 89)	23 (25.9%)	61 (68.5%)	5 (5.6%)	12 (13.5%)	52 (58.4%)	25 (28.1%)	<0.001

[b]Up-regulated: ratio of BaP treatment to DMSO greater than 1.5. Down-regulated: ratio less than 0.67.
[c]Percentages based on readable genes in respective gene categories.
[a] Chi-square test performed with 3 × 3 table.

Table 4
Differences in BaP effects on detoxification pathway between HepG2 and SCG2-1-1 cell lines

Group	BaP effects		Gene						
	HepG2 [a]	SCG2-1-1 [a]	Phase I		Phase II		Phase III		Total
A	Suppressed	Suppressed	3 EPHX2		2UGT2B10		0		5
			ALDH4		GSTA3				
			CYP51						
B	No difference	Suppressed	7 **CYP11B1** [b]	ALDH3B2	6**ACADSB** [b]	TST/RDS	6*ABCC3* [b]	ABCB8	19
			MAOA [b]	CYP2C8	*GSTM2* [b]	GSTM1	ABCD4	ABCF3	
			AKR1A1 [b]	CYP27B1	*UGT2B15* [b]		ABCF2	ABCA3	
			FMO5 [b]		SULT4A1				
C	No difference	No difference	22*ADH4* [b]	CBR1	13UGTREL1	GSTO1	7ABCB2		42
			CYP4F8 [b]	CYP2A6	GSTM4	UGT1A10	ABCB4		
			CYP26A1 [b]	CYP2B6	GSTZ1		ABCD1		
			ADH3	CYP2D6	ACADVL		ABCC5		
			AKR7A2	CYP3A5	GSTA4		ABCC8		
			AOX1	CYP17	ACADS		ABCC2		
			ALDH1A1	CYP24	ACADM		ABCF1		
			ALDH2	CYP27A1	COMT				
			ALDH3A2	CYP46A1	GSTT1				
			ALDH5A1	NQO2	MGST3				
			ADH7	MAOB	GSTA2				
D	Induced	Suppressed	0		1**SULT2A1** [b, c]		0		1
E	Induced	No difference	4 *CYP2J2* [c]	AKR1B1	4**MGST2** [b,c]	**UGT2B7** [b,c]	2**ABCB10** [b,c]		10
			CYP3A4 [c]	CES1 [b]	**SULT1A3** [b,c]	*GSTM3*	ABCB1 [b,c]		
F	Induced	Induced	9 **AKR1B10** [b]	*ALDH3A1* [b]	2GSTP1		1ABCB6 [b]		12
			CYP19 [b]	CYP1A1	MGST1				
			CYP39A1 [b,c]	CYP1A2 [c]					
			AKR1C1	EPHX1 [c]					
			AKR1C2						
Total			45		28		16		89

[a] Suppressed: ratio of BaP to DMSO less than 0.67. No difference: between 0.67 and 1.5. Induced: more than 1.5.
[b] Decreases greater than 2-fold in SCG2-1-1 to HepG2 are in bold; from 1.5- to 2-fold in italics.
[c] Genes classified by real-time PCR.

gene expression profiles (especially in liver detoxification pathways) and the role of GNMT in these processes.

We performed all of our hybridizations in triplicate for the accuracy and reliability. For cDNA hybridization, we labeled CRR (a pool of total RNA from 31 cell lines containing several cell types) with Cy3 and different samples with Cy5 for the purpose of making multiple comparisons of different sample combinations. Gene expression levels were averaged so as to avoid unexpected high or low levels.

BaP is a prototypical PAH that can be bioactivated into genotoxic metabolites by cytochrome P-450s (CYPs) and epoxide hydrolase; the result is the formation of covalent adducts with DNA (Harrigan et al., 2004). Bartosiewicz et al. (2001) used a DNA array containing 148 genes to show that BaP induced the up-regulation of only two genes (CYP1A1 and CYP1A2) and failed to induce significant increases in stress response genes or DNA repair genes. To our knowledge, the present study is the first to use a systematic approach to identify the effects of BaP on gene expression. For gene expression profile analysis, we used gene function as a parameter to create 13 groups (Table 1). The largest gene groups up-regulated by the BaP treatment of HepG2 cells were detoxification (13.9%), immune response (11.1%), and oncogenes (9.7%); the largest down-regulated gene groups were DNA repair (18.5%), cell cycle (18.3%), and tumor suppressor (16.3%). The up-regulation of detoxification pathway genes and down-regulation of DNA repair and cell cycle genes are considered important in the pathophysiology of BaP-treated cells. In addition, the up-regulation of oncogenes and down-regulation of tumor suppressor genes may play a role in BaP-induced tumorigenesis.

In terms of BaP–GNMT interaction, the detoxification pathway genes, kinase/phosphatase genes, and oncogenes experienced the greatest amounts of GNMT counteraction. This supports our previous finding that GNMT binds with BaP and inhibits BPDE-DNA adduct formation (Chen et al., 2004).

Of the detoxification pathway genes that we used in this study, 66.9% (89/133) were readable. The expression profiles of 21 were analyzed using real-time PCR; 76% (16/21) were verifiable. CYP1A2 expression levels were similar among the four samples in the microarray analysis but different according to our real-time PCR results. This disparity may be due to cross-hybridization reactions in the microarray analysis, which tended to underestimate the level of change of the gene transcripts in comparison to the real-time PCR data. This might also reflect an overestimation of the uninduced transcripts due to non-specific hybridization, or an underestimation of the level of induction due to the effects of probe saturation (Yuen et al., 2002). Following BaP treatment, GNMT was induced in HepG2; this may be due to the endogenous GNMT gene containing a predictive PAH responsive element (personal communication and Chen et al., 2000).

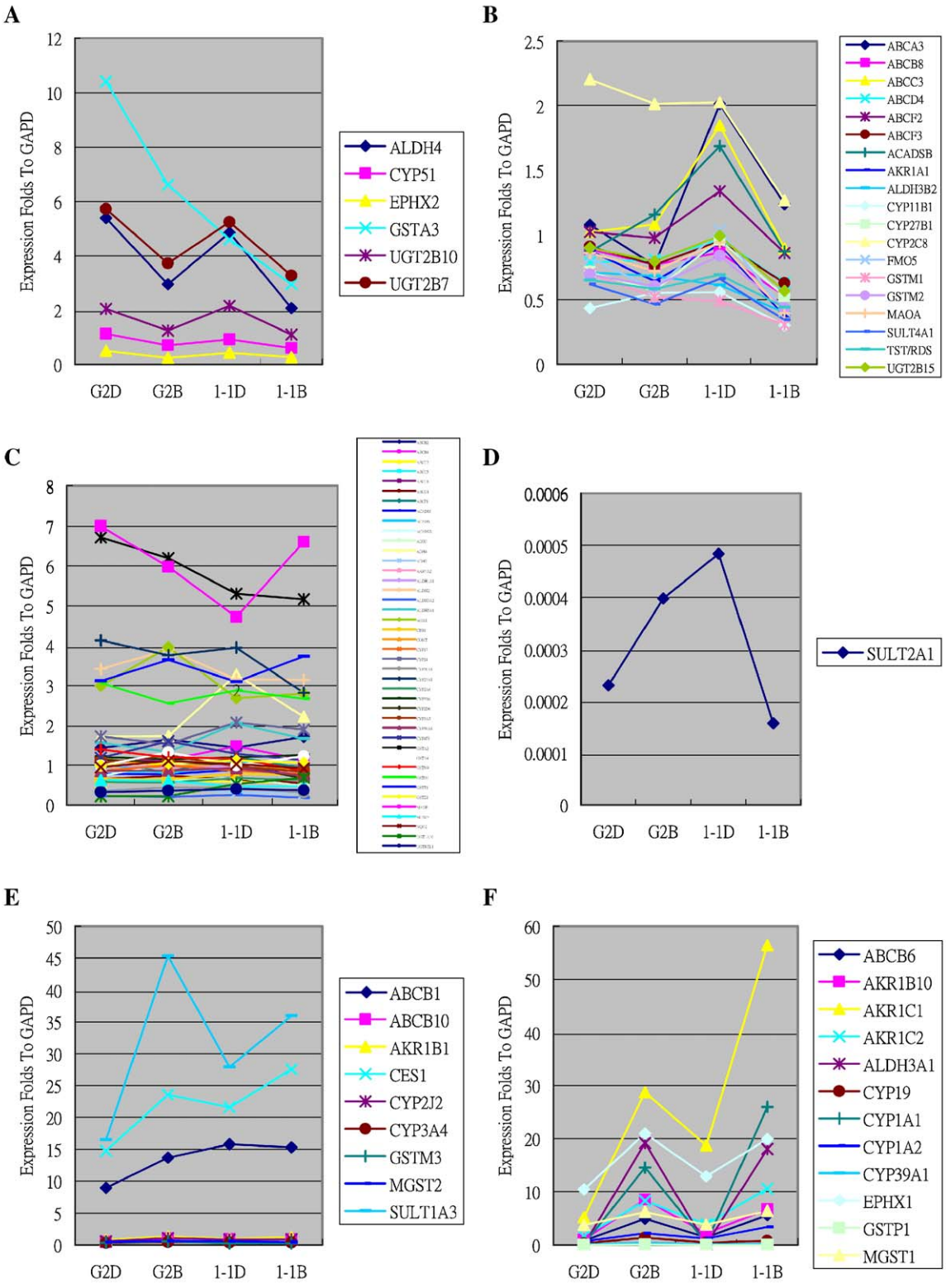

Fig. 3. Detoxification pathway gene expression pattern. Genes were placed in six categories according to BaP effects on detoxification gene expression levels in HepG2 and SCG2-1-1. A, both suppressed; B, no difference in HepG2, suppressed in SCG2-1-1; C, no difference in either; D, induced in HepG2 and suppressed in SCG2-1-1; E, induced in HepG2 and no difference in SCG2-1-1; F, both induced.

Previously, the following ten genes were found to be induced by PAH or BaP metabolites and no genes were found to be down-regulated by BaP: CYP1A1, CYP1A2, CYP1B1, AKR1C1, UGT2B7, ALDH3A1, UGT1A6, UGT1A9, NQO1 and GSTA1 (Bartosiewicz et al., 2001; Sladek, 2003; Burczynski et al., 1999; Wasserman and Fahl, 1997; Munzel et al.,

1999). In this study, we found that 5 of the 10 genes mentioned above which including CYP1A1, CYP1A2, AKR1C1, ALDH3A1 and UGT2B7 were induced by BaP in HepG2 cells. There were 23 genes that have never reported previously were found to be either up-regulated or down-regulated by BaP at least 1.5-folds, and AKR1C2, CYP3A4, CYP2J2 (phase I), GSTM3 (phase II), and ABCB1 (phase III) were found to be up-regulated at least 2-folds. There were 5 genes found to be down-regulated by BaP: EPHX2, ALDH4, CYP51 (phase I), UGT2B10 and GSTA3 (phase II).

The XRE-containing (xenobiotic responsive element) CYP1A1 and CYP1A2 genes were up-regulated in both HepG2 and SCG2-1-1 cells treated with BaP. CYP1A2 induction levels were similar between HepG2 and SCG2-1-1; in contrast, CYP1A1 increased 85.2-fold in HepG2/BaP and 68.8-fold in SCG2-1-1/BaP. The EpRE-containing (electrophile responsive element) AKR1C1 gene was up-regulated in the same two cell lines—5.5-fold in HepG2/BaP and 3.0-fold in SCG2-1-1/BaP. According to these results, GNMT counteracts CYP1A1 and AKR1C1 expression as induced by BaP. AKR1A1 is capable of oxidizing the metabolically relevant stereoisomers of PAH trans-dihydrodiols with high utilization ratios coupled with CYP1A1 and EH co-expression in PAH target tissues. Furthermore, it may play a major role in PAH activation in vivo (Palackal et al., 2001). No change in AKR1A1 gene expression was noted in HepG2/BaP, but it was down-regulated in SCG2-1-1/BaP. GNMT generally inhibited the effect of BaP on detoxification pathway genes.

Several UGTs (e.g., UGT2B7, UGT1A7, UGT1A8, UGT1A9, and UGT1A10) are known to exhibit glucuronidating activity against a number of phenolic BaP derivatives (Jin et al., 1993; Grove et al., 1997; Mojarrabi and Mackenzie, 1998; Guillemette et al., 2000). Furthermore, UGT1A1, UGT1A9, and UGT2B7 (all expressed in human liver cells) exhibit detectable levels of activity against benzo(a)pyrene-trans-7,8- dihydrodiol (BPD) isomers derived from BaP glucuronidation (Fang et al., 2002). Our data show that UGT2B7 was up-regulated by BaP in HepG2 and decreased the induction fold in SCG2-1-1.

In the present study, CYP1A1 was induced by BaP in a much larger scale than CYP3A4 in HepG2 cells (85.2-folds vs. 3.5-folds, Table 2). While in SCG2-1-1 cells, after BaP treatment, the folds of induction of CYP1A1 and CYP3A4 were reduced to 68.8 and 1.8 respectively. In addition, we found that antiporter genes were down-regulated in the presence of GNMT in our study. Buesen et al. (2002, 2003) used human intestinal Caco-2 cells to investigate BaP and BaP metabolite transportation, and found that BaP primarily metabolizes to B[a]P-1-sulfate and B[a]P-3-sulfate, both of which are subject to an apically directed transport that increases with CYP1A1 and CYP1B1 induction. In addition, many CYP3A substrates can act as ligands for phase III antiporter proteins (Wacher et al., 1995).

In an earlier study, we reported that when HepG2 cells were treated with 10 μM BaP, GNMT decreased BPDE-DNA adduct formation by 50% (Chen et al., 2004). The presence of GNMT significantly suppresses the effects of BaP, but does not eliminate them completely. In short, GNMT counteracts the effects of BaP on gene expression profiles. In the detoxification pathway, the expression levels of BaP-inducible genes (especially phase I and phase II genes) were reduced due to GNMT–BaP interaction. We therefore suggest that GNMT plays an important role in BaP detoxification pathway regulation.

Uncited reference

Liska, 1998

Acknowledgments

This work was supported by the National Research Program for Genomic Medicine of the National Science Council, Republic of China (Grant numbers NSC93-3112-B-010-003 and NSC93-3112-B-400-001) and grants from National Health Research Institutes to C. F. H. We thank Dr. Ming-Yi Chung (Taipei Veterans General Hospital) for her permission to use Applied Biosystems Prism 7700 sequence detection system; and members of the Division of Preventive Medicine of the Institute of Public Health at National Yang-Ming University for helpful feedback and technical support.

References

Aden, D.P., Fogel, A., Plotkin, S., Damjanov, I., Knowles, B.B., 1979. Controlled synthesis of HBsAg in a differentiated human liver carcinoma-derived cell line. Nature 282, 615–616.

Bartosiewicz, M., Penn, S., Buckpitt, A., 2001. Applications of gene arrays in environmental toxicology: fingerprints of gene regulation associated with cadmium chloride, benzo(a)pyrene, and trichloroethylene. Environ. Health Perspect. 109, 71–74.

Blumenstein, J., Williams, G.R., 1963. Glycine methyltransferase. Can. J. Biochem. Physiol. 41, 201–210.

Brazma, A., Hingamp, P., Quackenbush, J., Sherlock, G., Spellman, P., Stoeckert, C., Aach, J., Ansorge, W., Ball, C.A., Causton, H.C., Gaasterland, T., Glenisson, P., Holstege, F.C., Kim, I.F., Markowitz, V., Matese, J.C., Parkinson, H., Robinson, A., Sarkans, U., Schulze-Kremer, S., Stewart, J., Taylor, R., Vilo, J., Vingron, M., 2001. Minimum information about a microarray experiment (MIAME)-toward standards for microarray data. Nat. Genet. 29, 365–371.

Buesen, R., Mock, M., Seidel, A., Jacob, J., Lampen, A., 2002. Interaction between metabolism and transport of benzo[a]pyrene and its metabolites in enterocytes. Toxicol. Appl. Pharmacol. 183, 168–178.

Buesen, R., Mock, M., Nau, H., Seidel, A., Jacob, J., Lampen, A., 2003. Human intestinal Caco-2 cells display active transport of benzo[a]pyrene metabolites. Chem. Biol. Interact. 142, 201–221.

Burczynski, M.E., Lin, H.K., Penning, T.M., 1999. Isoform-specific induction of a human aldo-keto reductase by polycyclic aromatic hydrocarbons (PAHs), electrophiles, and oxidative stress: implications for the alternative pathway of PAH activation catalyzed by human dihydrodiol dehydrogenase. Cancer Res. 59, 607–614.

Chen, Y.M., Chen, L.Y., Wong, F.H., Lee, C.M., Chang, T.J., Yang-Feng, T.L., 2000. Genomic structure, expression, and chromosomal localization of the human glycine N-methyltransferase gene. Genomics 66, 43–47.

Chen, S.Y., Lin, J.R., Darbha, R., Lin, P., Liu, T.Y., Chen, Y.M., 2004. Glycine N-methyltransferase tumor susceptibility gene in the benzo(a)pyrene-detoxification pathway. Cancer Res. 64, 3617–3623.

Cook, R.J., Wagner, C., 1984. Glycine N-methyltransferase is a folate binding protein of rat liver cytosol. Proc. Natl. Acad. Sci. U.S.A. 81, 3631–3634.

Dearfield, K.L., Jacobson-Kram, D., Brown, N.A., Williams, J.R., 1983. Evaluation of a human hepatoma cell line as a target cell in genetic toxicology. Mutat. Res. 108, 437–449.

Denissenko, M.F., Cahill, J., Koudriakova, T.B., Gerber, N., Pfeifer, G.P., 1999.

Quantitation and mapping of aflatoxin B1-induced DNA damage in genomic DNA using aflatoxin B1-8,9-epoxide and microsomal activation systems. Mutat. Res. 425, 205–211.

Diamond, L., Kruszewski, F., Aden, D.P., Knowles, B.B., Baird, W.M., 1980. Metabolic activation of benzo[a]pyrene by a human hepatoma cell line. Carcinogenesis 1, 871–875.

Diamond, L., Cherian, K., Harvey, R.G., DiGiovanni, J., 1984. Mutagenic activity of methyl- and fluoro-substituted derivatives of polycyclic aromatic hydrocarbons in a human hepatoma (HepG2) cell-mediated assay. Mutat. Res. 136, 65–72.

Duthie, S.J., Coleman, C.S., Grant, M.H., 1988. Status of reduced glutathione in the human hepatoma cell line, HEP G2. Biochem. Pharmacol. 37, 3365–3368.

Eisen, M.B., Spellman, P.T., Brown, P.O., Botstein, D., 1998. Cluster analysis and display of genome-wide expression patterns. Proc. Natl. Acad. Sci. U.S. A. 95, 14863–14868.

Fang, J.L., Beland, F.A., Doerge, D.R., Wiener, D., Guillemette, C., Marques, M.M., Lazarus, P., 2002. Characterization of benzo(a)pyrene-trans-7,8-dihydrodiol glucuronidation by human tissue microsomes and overexpressed UDP-glucuronosyltransferase enzymes. Cancer Res. 62, 1978–1986.

Fukuda, Y., Ishida, N., Noguchi, T., Kappas, A., Sassa, S., 1992. Interleukin-6 down regulates the expression of transcripts encoding cytochrome P450 IA1, IA2 and IIIA3 in human hepatoma cells. Biochem. Biophys. Res. Commun. 184, 960–965.

Grant, M.H., Duthie, S.J., Gray, A.G., Burke, M.D., 1988. Mixed function oxidase and UDP-glucuronyltransferase activities in the human Hep G2 hepatoma cell line. Biochem. Pharmacol. 37, 4111–4116.

Grove, A.D., Kessler, F.K., Metz, R.P., Ritter, J.K., 1997. Identification of a rat oltipraz-inducible UDP-glucuronosyltransferase (UGT1A7) with activity towards benzo(a)pyrene-7,8-dihydrodiol. J. Biol. Chem. 272, 1621–1627.

Guengerich, F.P., 1992. Metabolic activation of carcinogens. Pharmacol. Ther. 54, 17–61.

Guillemette, C., Ritter, J.K., Auyeung, D.J., Kessler, F.K., Housman, D.E., 2000. Structural heterogeneity at the UDP-glucuronosyltransferase 1 locus: functional consequences of three novel missense mutations in the human UGT1A7 gene. Pharmacogenetics 10, 629–644.

Harrigan, J.A., Vezina, C.M., McGarrigle, B.P., Ersing, N., Box, H.C., Maccubbin, A.E., Olson, J.R., 2004. DNA adduct formation in precision-cut rat liver and lung slices exposed to benzo[a]pyrene. Toxicol. Sci. 77, 307–314.

Jin, C.J., Miners, J.O., Burchell, B., Mackenzie, P.I., 1993. The glucuronidation of hydroxylated metabolites of benzo[a]pyrene and 2-acetylaminofluorene by cDNA-expressed human UDP-glucuronosyltransferases. Carcinogenesis 14, 2637–2639.

Josephy, P.D., 1997. Polycyclic aromatic hydrocarbon carcinogenesis. In: Josephy, P.D., Mannervik, B., Ortiz de Montellano, P.R. (Eds.), Molecular Toxicology. Oxford Univ. Press, New York, pp. 334–347.

Kerr, S.J., 1972. Competing methyltransferase systems. J. Biol. Chem. 247, 4248–4252.

Knowles, B.B., Howe, C.C., Aden, D.P., 1980. Human hepatocellular carcinoma cell lines secrete the major plasma proteins and hepatitis B surface antigen. Science 209, 497–499.

Limbosch, S., 1983. Benzo[a]pyrene- and aldrin-metabolizing activities in cultured human and rat hepatoma cell lines. J. Natl. Cancer Inst. 71, 281–286.

Liska, D.J., 1998. The detoxification enzyme systems. Altern. Med. Rev. 3, 187–198.

Lloyd, D.R., Hanawalt, P.C., 2000. p53-dependent global genomic repair of benzo[a]pyrene-7,8-diol-9,10-epoxide adducts in human cells. Cancer Res. 60, 517–521.

Mojarrabi, B., Mackenzie, P.I., 1998. Characterization of two UDP glucuronosyltransferases that are predominantly expressed in human colon. Biochem. Biophys. Res. Commun. 247, 704–709.

Munzel, P.A., Schmohl, S., Heel, H., Kalberer, K., Bock-Hennig, B.S., Bock, K.W., 1999. Induction of human UDP glucuronosyltransferases (UGT1A6, UGT1A9, and UGT2B7) by t-butylhydroquinone and 2,3,7,8-tetrachlorodibenzo-p-dioxin in Caco-2 cells. Drug Metab. Dispos. 27, 569–573.

Palackal, N.T., Burczynski, M.E., Harvey, R.G., Penning, T.M., 2001. Metabolic activation of polycyclic aromatic hydrocarbon trans-dihydrodiols by ubiquitously expressed aldehyde reductase (AKR1A1). Chem. Biol. Interact. 130–132, 815–824.

Sassa, S., Sugita, O., Galbraith, R.A., Kappas, A., 1987. Drug metabolism by the human hepatoma cell, Hep G2. Biochem. Biophys. Res. Commun. 143, 52–57.

Shimada, T., Yun, C.H., Yamazaki, H., Gautier, J.C., Beaune, P.H., Guengerich, F.P., 1992. Characterization of human lung microsomal cytochrome P-450 1A1 and its role in the oxidation of chemical carcinogens. Mol. Pharmacol. 41, 856–864.

Sladek, N.E., 2003. Human aldehyde dehydrogenases: potential pathological, pharmacological, and toxicological impact. J. Biochem. Mol. Toxicol. 17, 7–23.

Sokal, R.R., Michener, C.D., 1958. Univ. Kans. Sci. Bull. 38, 1409–1438.

Wacher, V.J., Wu, C.Y., Benet, L.Z., 1995. Overlapping substrate specificities and tissue distribution of cytochrome P450 3A and P-glycoprotein: implications for drug delivery and activity in cancer chemotherapy. Mol. Carcinog. 13, 129–134.

Wani, M.A., Zhu, Q., El Mahdy, M., Venkatachalam, S., Wani, A.A., 2000. Enhanced sensitivity to anti-benzo(a)pyrene-diol-epoxide DNA damage correlates with decreased global genomic repair attributable to abrogated p53 function in human cells. Cancer Res. 60, 2273–2280.

Wasserman, W.W., Fahl, W.E., 1997. Functional antioxidant responsive elements. Proc. Natl. Acad. Sci. U.S.A. 94, 5361–5366.

Yuen, T., Wurmbach, E., Pfeffer, R.L., Ebersole, B.J., Sealfon, S.C., 2002. Accuracy and calibration of commercial oligonucleotide and custom cDNA microarrays. Nucleic Acids Res. 30, e48.